Preprints of the 21st IFAC World Congress (Virtual)
Berlin, Germany, July 12-17, 2020

Control of an Underactuated 4 Cable-Driven Parallel Robot using Modified Input-Output Feedback Linearization

Atal Anil Kumar*, Jean-François Antoine*
Gabriel Abba*

** Université de Lorraine, Arts et Metiers Institute of Technology, LCFC, HESAM Université, F-57070 Metz, France (e-mails: atal-anil.kumar@univ-lorraine.fr, jean-francois.antoine@univ-lorraine.fr, gabriel.abba@univ-lorraine.fr)*

Abstract: This paper presents the control of an underactuated four Cable-Driven Parallel Robot (CDPR) using a modified input-output feedback linearization technique. The effect of internal dynamics (due to the underactuated degrees of freedom of the CDPR) on the behavior of the moving platform is presented to highlight the need of an improved controller to stabilize the system outputs. A modified control scheme is then proposed as a solution to obtain stable system outputs. A structure with two separate branches is modeled to simultaneously act on the control inputs and the mathematical calculations are done using the well-established equations of nonlinear control theory. Following this, the response of the system to the modified control law is then verified by simulation. A comparison between the classical and modified feedback linearization is shown to illustrate the significant improvement in the stabilization of the various parameters such as the cable tensions and platform orientations.

Keywords: Underactuated CDPR, Input-output feedback linearization, Internal dynamics, nonlinear control, stability.

1. INTRODUCTION

Cable-Driven Parallel Robots (CDPRs) is a special variant of traditional parallel robots in which the moving platform (MP) is connected to the base frame by a set of cables whose lengths are adjusted by actuated winches. Coordinated retraction and extension of cables control the position and orientation of the platform (Merlet and Daney, 2010). One of the important challenges in the design of the CDPRs arises from the fact that cables can only pull and not push. As a result of this, a unilateral constraint exists in which the cables must always be maintained in tension, thus, resulting in a larger number of cables in general than the number of degrees of freedom (DoF) to fully restrain or control the moving platform (Ming, 1994).

A CDPR is said to be underactuated if the number of actuators employed for the control of the MP is less than its DoF. Such CDPRs have at most one feasible solution for cable tensions and mostly rely on gravity for keeping the cables taut. Application of underactuated CDPRs with a limited number of cables can be found in tasks requiring a limited number of controlled DoFs or when a limitation of dexterity is acceptable in order to decrease complexity, cost, set-up time, the likelihood of cable interference, etc. (Abbasnejad and Carricato, 2015)

While a rich literature is available describing the control of fully and over-constrained CDPRs (Alp and Agrawal, 2002; Oh and Agrawal, 2006; Zi et al., 2008), very few works are available on the control of underactuated CDPRs. Some of the approaches are dynamic trajectory planning (Gosselin et al., 2012), anti-sway trajectory generation based on input-shaping (Park et al., 2013), zero-vibration input shaping scheme (Hwang et al., 2016), flatness-based control (Heyden and Woernle, 2006), rest-to-rest trajectory planning (Ida et al., 2019), and so on.

The application of classical input-output feedback linearization has been presented in (Kumar et al., 2019a). However, the work did not show the effect of internal dynamics on the platform behavior at various points. The main contribution of this work is to present the effects of internal dynamics on the MP and to propose a modified feedback linearization control to stabilize the values of cables tensions which in turn helps in stabilizing the DoFs of the moving platform (mainly the platform orientations). The simulation results indicate that the modified control law performs significantly better than the classical I/O feedback linearization and can be implemented in the real prototype for validation.

The paper is organized as follows: Section 2 presents the dynamic model of the CDPR followed by section 3 which introduces the input-output feedback linearization in general. The effect of internal dynamics on the CDPR is shown in section 4. The concept of the modified control law is presented in section 5 followed by the simulation results comparing both the control laws in section 6.

2. DYNAMIC MODEL OF THE CDPR

The modelling and analysis methods developed for conventional rigid link manipulators cannot be directly applied to the cable-driven robots because of the unilateral constraints where the tensions in the cables must be considered.

A general sketch of cable-driven parallel robot is shown in (Fig. 1).

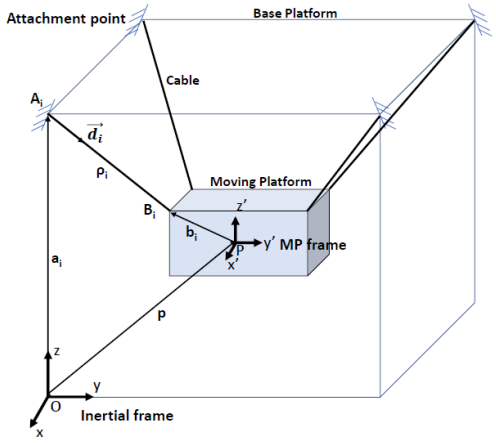

Fig. 1: Simple sketch of one of the cables of the CDPR

A fixed reference frame (*O, x, y, z*) attached to the base of a CDPR is referred to as the base frame. A moving reference frame (*P, x', y', z'*) is attached to the mobile platform where *P* is the reference point of the platform to be positioned by the mechanism. From (fig. 1), a_i and b_i are respectively defined as the vector connecting point *O* to point A_i and the vector connecting point *P* of the platform to the point B_i, both vectors being expressed in the base frame. The position *p* of the mobile platform is given by $\overrightarrow{OP}$. In order to reduce the complexity of computation in modelling, we assume the following (Gosselin, 2014):

1) The mass of the cables is negligible and the cables are non-elastic.
2) The i^{th} cable is assumed to be taut between points and is therefore considered a straight segment and is denoted by ρ_i.
3) The moving platform is assumed to be a rigid body, defined by its mass and inertia matrix.

The equations of motion for a CDPR can be derived using Newton–Euler formulations provided all cables are in tension as shown in (1) (Begey et al., 2019).

$$\begin{bmatrix} mI_{3\times3} & 0_{3\times3} \\ 0_{3\times3} & I_P \end{bmatrix}\begin{bmatrix} \ddot{p} \\ \dot{\omega} \end{bmatrix} + \begin{bmatrix} 0_{3\times1} \\ \omega \times I_P\omega \end{bmatrix} + \begin{bmatrix} -mg \\ 0_{3\times1} \end{bmatrix} = -J^T\tau \qquad (1)$$

In this equation, *m* denotes the mass of the moving platform with the payload, I_P is a 3×3 matrix and denotes the inertia tensor of the end-effector about point *P* in the base frame, $I_{3\times3}$ is a 3×3 identity matrix, *g* denotes the gravity acceleration vector, τ denotes the vector of cables forces while scalar t_i denotes the tension force of the i^{th} cable, $\omega = [\omega_x, \omega_y, \omega_z]^T$ denotes the velocity vector of the orientation, $p = [p_x, p_y, p_z]^T$ denotes the position vector. Consider $X = [x, y, z, \alpha, \beta, \gamma]^T$ as generalized coordinates vector, in which $\theta = [\alpha, \beta, \gamma]^T$ denotes the vector of a set of Euler angles. With this definition, the rotation matrix can be written in terms of Euler angles as:

$$R = \begin{bmatrix} c\beta c\gamma & c\gamma s\alpha s\beta - c\alpha s\gamma & c\alpha c\gamma s\beta + s\alpha s\gamma \\ c\beta s\gamma & c\alpha c\gamma + s\alpha s\beta s\gamma & -c\gamma s\alpha + c\alpha s\beta s\gamma \\ -s\beta & c\beta s\alpha & c\alpha c\beta \end{bmatrix} \qquad (2)$$

where, *s* and *c* represent *sin* and *cos* functions, respectively. The angular velocity of the end-effector can be written in the following form,

$$\omega = E\dot{\theta} \qquad (3)$$

$$\dot{\theta} = [\dot{\alpha}, \dot{\beta}, \dot{\gamma}]^T \qquad (4)$$

in which,

$$E = \begin{bmatrix} \mathrm{c}\beta\mathrm{c}\gamma & -\mathrm{s}\gamma & 0 \\ \mathrm{c}\beta\mathrm{s}\gamma & \mathrm{c}\gamma & 0 \\ -\mathrm{s}\beta & 0 & 1 \end{bmatrix} \qquad (5)$$

The equations of motion can be written in terms of *X* using the notations defined above. By some manipulations these equations may be derived as,

$$M(X)\ddot{X} + C(X, \dot{X})\dot{X} + G(X) = -J^T\tau \qquad (6)$$

where,

$$M(X) = \begin{bmatrix} mI_{3\times3} & 0_{3\times3} \\ 0_{3\times3} & I_PE \end{bmatrix}$$

$$C(X, \dot{X}) = \begin{bmatrix} 0_{3\times3} & 0_{3\times3} \\ 0_{3\times3} & I_P\dot{E} + (E\dot{\theta})_\times(I_PE) \end{bmatrix}$$

$$G(X) = \begin{bmatrix} -mg \\ 0_{3\times1} \end{bmatrix}$$

in which, the matrix $(E\dot{\theta})_\times$ is a skew-symmetric matrix defined by the components of the angular velocity vector as

The Jacobian transpose of the CDPR is given by

$$J^T = \begin{bmatrix} d_1^O & \dots & d_i^O & \dots \\ b_1^O \times d_1^O & \dots & b_i^O \times d_i^O & \dots \end{bmatrix} \qquad (7)$$

where, d_i^O is the unit vector giving the direction of the i^{th} cable from its end point on the base frame *(O)* to its end point on the MP and b_i^O is the vector from the MP centre of gravity *P* to the end point B_i expressed in the inertial frame.

Equation (6) is finally represented as

$$M(X)\ddot{X} + N(X, \dot{X})\dot{X} = -J^T\tau \qquad (8)$$

where, $N(X, \dot{X})\dot{X} = C(X, \dot{X})\dot{X} + G(X)$

Equation (8) is then used for the implementation of the input-output feedback linearization method.

3. INPUT-OUTPUT FEEDBACK LINEARIZATION

The mathematical approach of the input-output feedback linearization (I/O FL) method for a nonlinear MIMO dynamic system of n^{th} order with m number of inputs and outputs is presented in this section. Further explanation of the technique in detail can be found in (Isidori, 2013). Consider a MIMO system described in the affine form as given below:

$$\dot{x}(t) = f(x,t) + g_1(x,t)u_1(t) + \cdots + g_m(x,t)u_m(t) \quad (9)$$

$$y_1(t) = h_1(x,t)$$
$$\cdots$$
$$y_m(t) = h_m(x,t)$$

where, $i = 1..m - i^{th}$ inputs, $j=1..m - j^{th}$ outputs, $x(t) \in R^n$ is state vector, $u_i(t)$ is control input, $y_j(t)$ is the system output, $f(x,t)$, $g_i(x,t)$ and $h_j(x,t)$ are smooth nonlinear functions.

The basic principle of the input-output feedback linearization method is in finding an input transformation in the shape

$$u_i = \alpha_i(x) + \beta_i(x)v_i \quad (10)$$

Where v_i is the new input, $\alpha_i(x), and, \beta_i(x)$ are nonlinear functions.

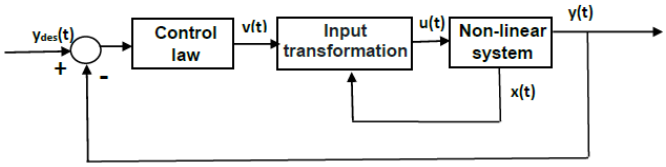

Fig. 2: Block diagram representation of the input-output linearization

Equation (10) helps in creating a linear relationship among the outputs y_i and the new inputs v_i decoupling the interaction between the original inputs and outputs. Following this decoupling, control algorithms for each subsystem with input and output independent of each other can be synthesized using the conventional linear control laws. In order to achieve this, each output is repeatedly differentiated until the input signals appear in the expression of derivation. The individual derivatives of outputs are calculated using lie derivatives which are marked as $L_f h$ and $L_g h$. The first derivative has the form

$$\dot{y_J} = L_f h_j(x) + \sum_{i=1}^{m} L_{g_i} h_j(x) u_i \quad (11)$$

where, $L_f h_j(x) = \frac{\partial h_j}{\partial x} f(x),\ L_{g_i} h_j(x) = \frac{\partial h_j}{\partial x} g_i(x)$

If the expression $L_{g_i} h_j(x) = 0$ for all i,, it means that the inputs have not appeared in the derivation making it necessary to continue with the differentiation process till at least one input appears in the derivation. The resulting derivation takes the form

$$y_j^{r_j} = L_f^{r_j} h_j(x) + \sum_{i=1}^{m} L_{g_i} L_f^{r_j - 1} h_j(x) u_i \quad (12)$$

where, r_j represents the number of derivatives needed for at least one of the inputs to appear, also known as the relative order.

This approach is followed for each output y_j. The resulting m equations can be written in the form

$$\begin{bmatrix} y_1^{r_1} \\ \cdots \\ y_m^{r_m} \end{bmatrix} = \begin{bmatrix} L_f^{r_1} h_1(x) \\ \cdots \\ L_f^{r_m} h_m(x) \end{bmatrix} + E(x) \begin{bmatrix} u_1 \\ \cdots \\ u_m \end{bmatrix} \quad (13)$$

where $E(x)$ is a $m \times m$ matrix of shape

$$E(x) = \begin{bmatrix} L_{g_1} L_f^{r_1 - 1} h_1 & \cdots & L_{g_m} L_f^{r_1 - 1} h_1 \\ \vdots & \ddots & \vdots \\ L_{g_1} L_f^{r_m - 1} h_m & \cdots & L_{g_m} L_f^{r_m - 1} h_m \end{bmatrix}$$

If the matrix $E(x)$ is regular, then it is possible to define the input transformation in the shape

$$\begin{bmatrix} u_1 \\ \vdots \\ u_m \end{bmatrix} = -E^{-1}(x) \begin{bmatrix} L_f^{r_1} h_1(x) \\ \vdots \\ L_f^{r_m} h_m(x) \end{bmatrix} + E^{-1}(x) \begin{bmatrix} v_1 \\ \vdots \\ v_m \end{bmatrix} \quad (14)$$

Once the input transformation is completed as shown in (14) the linear control law is used to propose a feedback control for the linear system to ensure the desired behaviour of the nonlinear system using the conventional techniques. The relative degree (r_i) of the individual output is then used to calculate the overall vector relative degree of the system (r) to analyze the concept of internal dynamics.

$$r = r_1 + r_2 + \cdots + r_m \quad (15)$$

From equation (15), we will be able to calculate to vector relative degree of the system (r). If the vector relative degree is less than the number of states of the system (n), there exists internal dynamics (ID) in the system. In order to apply the classical I/O feedback linearization, it is important to study the effect of ID on the overall behaviour of the system.

4. PRELIMINARY APPLICATION OF INPUT-OUTPUT FEEDBACK LINEARIZATION FOR A CDPR MODEL

The dynamic model (8) of the CDPR can be represented as shown follows:

$$\underline{\dot{X}} = F + Gu \quad (16)$$

$$\underline{y} = h(\underline{X})$$

where, $\underline{X} = \begin{Bmatrix} X \\ \dot{X} \end{Bmatrix}, F = \begin{Bmatrix} \dot{X} \\ -M^{-1}N \end{Bmatrix}, G = \begin{Bmatrix} 0_{6\times 1} \\ -M^{-1}J^T \end{Bmatrix}$

with constraints, $0 \le u \le u_{max}$

The input vector u of the system is given by the forces in the four cables (u_1, u_2, u_3, u_4) while the output of the system ($\underline{y}$) is

the position of the platform *(x,y,z)* and one of the angle namely, *gamma (γ),* which is the orientation angle about the z-axis.

The application of classical input-output feedback linearization for a CDPR model can be found in (Kumar et al., 2019a). From the preliminary calculation and simulation of the model, it has been found that the considered CDPR has a vector relative degree (*r*) of 8 while the total states of the system (*n*) are 12. Hence, this indicates the presence of internal dynamics (of 4 states); the effect of which has to be checked for the application of the control law.

In order to visualise the effect of internal dynamics, the I/O feedback linearization control was applied on the CDPR model with the conditions as mentioned in (Kumar et al., 2019a). The corresponding values of *α, β, γ* for the starting and final point is calculated from the static equilibrium program developed by the authors in (Kumar et al., 2019b). A quintic polynomial was used to generate the desired trajectory to obtain smooth values for the acceleration and velocity.

Table 1: Simulation parameters for the control laws

Room dimension (m)	5*5*3
Platform dimension (m)	0.5*0.5*0.2
Max. and Min. cable tension (N)	500N and 1N respectively
Starting point*(t=0)*	*x=2, y=0.5, z=1.5*
Final point*(t=10)*	*x=2, y=2, z=1.5*
Mass of the platform including the object weight	*30kg*

Table 2: Cable attachment points for centre of mass at a height of 1.5m from bottom

Cable no.	MP	Base
Cable 1	[2.25,2.25,1.7]	[0,0,3]
Cable 2	[2.25,2.75,1.7]	[0,5,3]
Cable 3	[2.75,2.75,1.7]	[5,5,3]
Cable 4	[2.75,2.25,1.7]	[5,0,3]

The results of the simulation are shown in fig. (3) and (4). It can be seen from the figure that the internal dynamics results in oscillatory behaviour in the uncontrolled DoFs which in turn leads to high variations in the tensions produced in the cable. On further analysis, it is found that the oscillatory behaviour is profound as the value of the platform orientation about x and y axis increases, indicating that as the MP moves closer to the boundary of the room it is affected more by the ID.

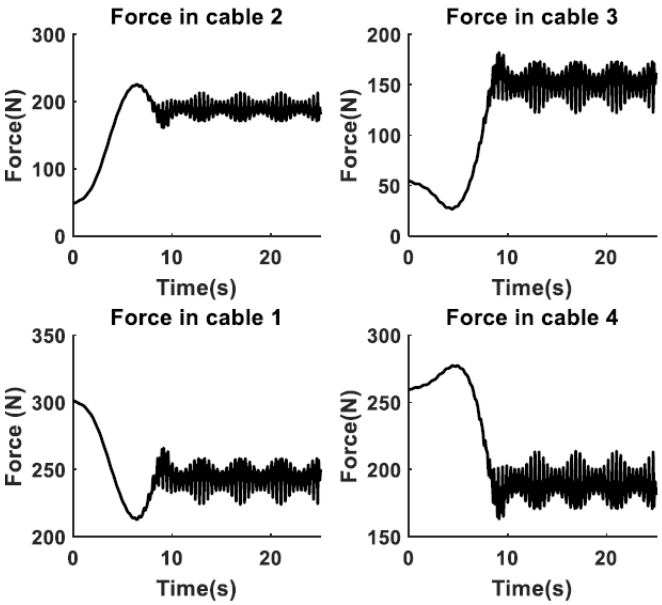

Fig. 3: Cable forces because of the internal dynamics in the underactuated CDPR

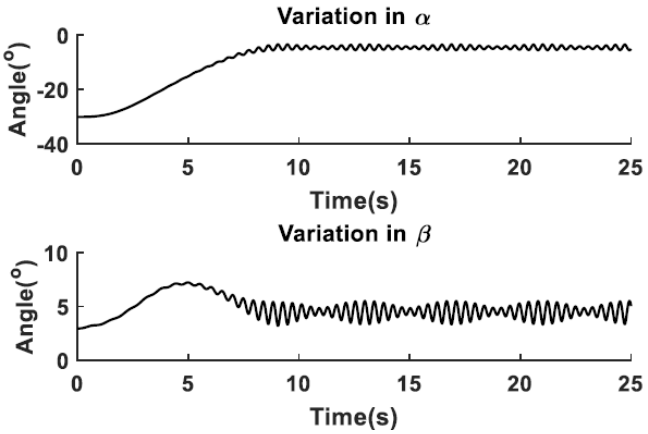

Fig. 4: Oscillations in the uncontrolled DoFs (α and β)

It is also observed from simulations that the classical I/O feedback linearization is not able to generate positive cable tensions at some points in the room because of their underactuated behaviour. One example of such situation is when the MP is moved from x=0.6, y=0.6, z=1.5 to x=2, y=2, z=1.5. A more thorough analysis to quantify the region of controllable workspace (points in the room where the control law can be applied with positive cable tensions and stabilized system outputs) will be done in the forthcoming work.

5. MODIFIED INPUT-OUTPUT FEEDBACK LINEARIZATION

A modified input-output feedback linearization approach has been proposed in this section to reduce the effect of oscillatory internal dynamics and stabilize the system behaviour.

The proposed approach uses the regular I/O feedback linearization as its foundation; however, it is divided into two separate branches which acts simultaneously on the control

input i.e., the tensions in the cables. The external forces acting on each branch is divided by 2 to calculate the control inputs from each branch. The block diagram of the proposed modification is as shown below:

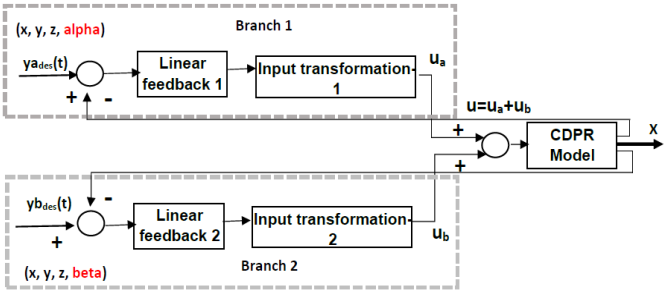

Fig. 5: Block diagram representation of the modified input-output linearization

Equation (16) is used to model the proposed law. However, the outputs to be controlled in the two branches are as

$$\underline{y_{a1}} = x, \underline{y_{a2}} = y, \underline{y_{a3}} = z, \underline{y_{a4}} = \alpha \qquad (17)$$

$$\underline{y_{b1}} = x, \underline{y_{b2}} = y, \underline{y_{b3}} = z, \underline{y_{b4}} = \beta \qquad (18)$$

Following this, the individual values of the input forces (u_a and u_b) corresponding to the branch *1 & 2* is calculated by following the steps shown in section 3, eq (11-14).The final input vector u is then calculated as the sum of the individual contribution from the two branches shown in the block diagram i.e.,

$$u = u_a + u_b \qquad (19)$$

where, u_a and u_b are the values of the forces calculated from the individual corresponding branches (1 & 2) as shown in the block diagram.

6. SIMULATION OF THE CONTROL LAW

The results of the simulation (using MATLAB) demonstrating the effectiveness of the modified control law over the classical I/O feedback linearization is presented in this section. The simulation conditions are mentioned in table 1. The initial and final values of alpha and beta are calculated from the static equilibrium conditions. The desired trajectory points are generated using a quantic polynomial as before. The results obtained are presented in fig. (5) and (6). The cable forces generated by the modified control law to follow the desired trajectory is shown in fig. (5). It is seen that the values of the forces are positive and within the limits defined in table 1. Figure 6 shows the comparison of the platform orientation values generated by the modified control law and the classical I/O feedback linearization. It is clearly visible that the orientation values are more stable with the application of modified feedback linearization. Both the control laws however have satisfactory behaviour to control the position of the MP.

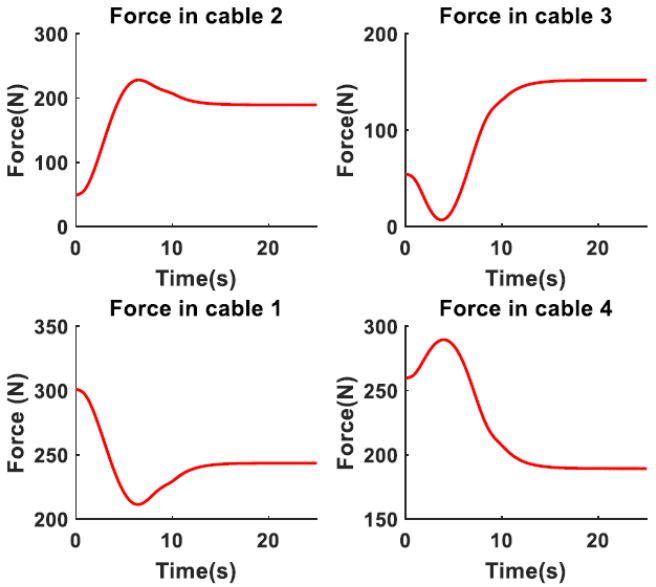

Fig. 5: Cable forces using the modified input-output feedback linearization

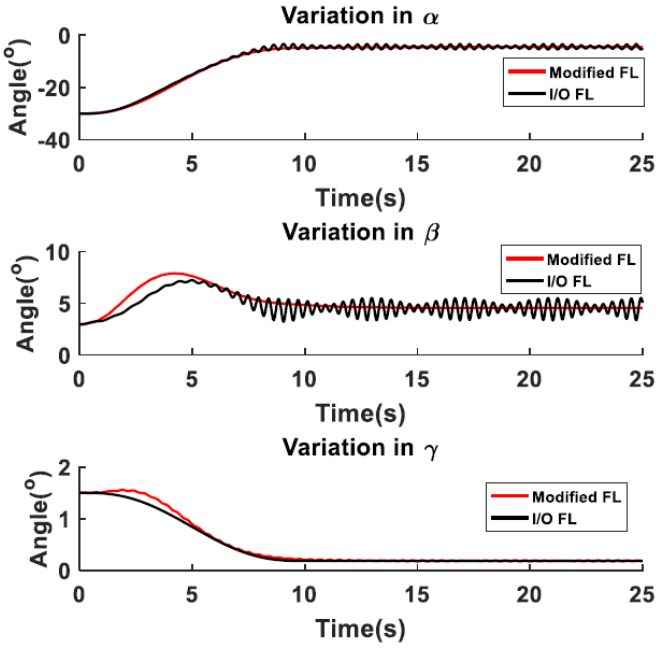

Fig. 6: Variation of platform orientations with modified I/O FL and classical I/O FL respectively

As mentioned in section 4, the classical I/O FL fails to generate positive values of cable tensions (force in cable 3) for moving the cable from specific points. The modified control law was tested for the same starting points using the same trajectory to be followed. For the points considered, it is observed that positive tension values were generated in all the four cables. Figure 7 shows the value of the forces in cable 3 for the simulation. As said before, I/O FL generated negative tensions in the cable to achieve the trajectory, but the modified FL was successful in generating positive cable tensions. The values of the forces are

Tension in cable 3 (I/O FL) = **- 41.88 N (<0)**
Tension in cable 3 (Modified FL) = + **17.59 N (>0)**

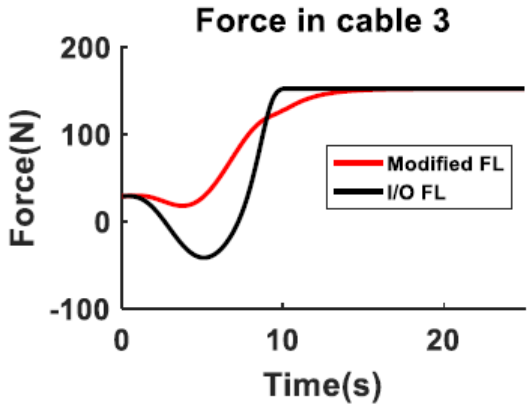

Fig. 7: Force in cable 3 showing negative cable tension for I/O FL and positive cable tension for Modified FL

Hence, it is evident from the simulations that the modified control law has the potential to improve the controllable workspace of the underactuated CDPR. The quantification of this will be done in further works.

7.CONCLUSION

This article demonstrated the implementation of a modified input-output feedback linearization method to control an underactuated cable-driven parallel robot. The simulation results proved that the proposed control law stabilized the system output significantly and can be tested on the real prototype. It was also shown that the proposed control law might also impact the controllable workspace of the CDPR. However, the application of the modified control law for different configurations needs to be investigated for better validation and formulation of the stability conditions. Also, experiments will be conducted on the prototype which is being prepared for real-time validation of the control law. In the end, the cable elasticity will also be included in the control law to provide a robust solution for the operation of underactuated CDPRs.

ACKNOWLEDGEMENT

We would like to thank the Robotix Academy for funding this work as a part of the project funded by INTERREG V-A Grand Region program.

REFERENCES

Abbasnejad, G., Carricato, M., 2015. Direct Geometrico-static Problem of Underconstrained Cable-Driven Parallel Robots With n Cables. IEEE Trans. Robot. 31, 468–478.

Alp, A.B., Agrawal, S.K., 2002. Cable suspended robots: Feedback controllers with positive inputs, in: American Control Conference, 2002. Proceedings of the 2002. IEEE, pp. 815–820.

Begey, J., Cuvillon, L., Lesellier, M., Gouttefarde, M., Gangloff, J., 2019. Dynamic Control of Parallel Robots Driven by Flexible Cables and Actuated by Position-Controlled Winches. IEEE Trans. Robot. 35, 286–293.

Gosselin, C., 2014. Cable-driven parallel mechanisms: state of the art and perspectives. Mech. Eng. Rev. 1, DSM0004–DSM0004.

Gosselin, C., Ren, P., Foucault, S., 2012. Dynamic trajectory planning of a two-DOF cable-suspended parallel robot, in: Robotics and Automation (ICRA), 2012 IEEE International Conference On. IEEE, pp. 1476–1481.

Heyden, T., Woernle, C., 2006. Dynamics and flatness-based control of a kinematically undetermined cable suspension manipulator. Multibody Syst. Dyn. 16, 155–177.

Hwang, S.W., Bak, J.-H., Yoon, J., Park, J.H., Park, J.-O., 2016. Trajectory generation to suppress oscillations in under-constrained cable-driven parallel robots. J. Mech. Sci. Technol. 30, 5689–5697.

Ida, E., Bruckmann, T., Carricato, M., 2019. Rest-to-Rest Trajectory Planning for Underactuated Cable-Driven Parallel Robots. IEEE Trans. Robot. 1–14.

Isidori, A., 2013. Nonlinear control systems, Third edition, softcover reprint of the hardcover 3rd edition 2000. ed, Communications and control engineering. Springer, London.

Kumar, A.A., Antoine, J.-F., Abba, G., 2019a. Input-Output Feedback Linearization for the Control of a 4 Cable-Driven Parallel Robot. IFAC-Pap. 52, 707–712.

Kumar, A.A., Antoine, J.-F., Zattarin, P., Abba, G., 2019b. Workspace Analysis of a 4 Cable-Driven Spatial Parallel Robot, in: Arakelian, V., Wenger, P. (Eds.), ROMANSY 22 – Robot Design, Dynamics and Control. Springer International Publishing, Cham, pp. 204–212.

Merlet, J., Daney, D., 2010. A portable, modular parallel wire crane for rescue operations, in: Robotics and Automation (ICRA), 2010 IEEE International Conference On. IEEE, pp. 2834–2839.

Ming, A., 1994. Study on Multiple Degree-of-Freedom Positioning Mechanism Using Wires (Part I)-Concept, Design and Control. Int. J. Jpn. Soc. Precis. Eng. 28, 131–138.

Oh, S.-R., Agrawal, S.K., 2006. Generation of feasible set points and control of a cable robot. IEEE Trans. Robot. 22, 551–558.

Park, J., Kwon, O., Park, J.H., 2013. Anti-sway trajectory generation of incompletely restrained wire-suspended system. J. Mech. Sci. Technol. 27, 3171–3176.

Zi, B., Duan, B.Y., Du, J.L., Bao, H., 2008. Dynamic modeling and active control of a cable-suspended parallel robot. Mechatronics 18, 1–12.